

# Prevention of neonatal oxygen-induced brain damage by reduction of intrinsic apoptosis

M Siffringer<sup>\*,1,2,7</sup>, I Bendix<sup>3,7</sup>, C Börner<sup>2</sup>, S Endesfelder<sup>2</sup>, C von Haefen<sup>1</sup>, A Kalb<sup>1</sup>, S Holifanjaniaina<sup>4,5</sup>, S Prager<sup>3</sup>, GW Schlager<sup>3</sup>, M Keller<sup>3</sup>, E Jacotot<sup>4,5,6</sup> and U Felderhoff-Mueser<sup>3</sup>

Within the last decade, it became clear that oxygen contributes to the pathogenesis of neonatal brain damage, leading to neurocognitive impairment of prematurely born infants in later life. Recently, we have identified a critical role for receptor-mediated neuronal apoptosis in the immature rodent brain. However, the contribution of the intrinsic apoptotic pathway accompanied by activation of caspase-2 under hyperoxic conditions in the neonatal brain still remains elusive. Inhibition of caspases appears a promising strategy for neuroprotection. In order to assess the influence of specific caspases on the developing brain, we applied a recently developed pentapeptide-based group II caspase inhibitor (5-(2,6-difluorophenoxy)-3(R,S)-(2(S)-(2(S)-(3-methoxycarbonyl-2(S)-(3-methyl-2(S)-((quinoline-2-carbonyl)-amino)-butyrylamino)propionylamino)3-methylbutyrylamino)propionylamino)-4-oxo-pentanoic acid methyl ester; TRP601). Here, we report that elevated oxygen (hyperoxia) triggers a marked increase in active caspase-2 expression, resulting in an initiation of the intrinsic apoptotic pathway with upregulation of key proteins, namely, cytochrome *c*, apoptosis protease-activating factor-1, and the caspase-independent protein apoptosis-inducing factor, whereas BH3-interacting domain death agonist and the anti-apoptotic protein B-cell lymphoma-2 are downregulated. These results coincide with an upregulation of caspase-3 activity and marked neurodegeneration. However, single treatment with TRP601 at the beginning of hyperoxia reversed the detrimental effects in this model. Hyperoxia-mediated neurodegeneration is supported by intrinsic apoptosis, suggesting that the development of highly selective caspase inhibitors will represent a potential useful therapeutic strategy in prematurely born infants.

*Cell Death and Disease* (2012) 3, e250; doi:10.1038/cddis.2011.133; published online 12 January 2012

**Subject Category:** Neuroscience

The number of infants born prematurely has substantially increased in the last two decades, with a worldwide rate of 9.6%. Substantial neurological morbidity may occur in survivors of preterm birth.<sup>1,2</sup> In recent years, experimental studies revealed that oxygen, which is widely used in neonatal intensive care to treat respiratory distress, triggers a disruption of intracellular redox homeostasis. This disturbance can lead to oxidative and nitrate stress, resulting in increased neuronal and oligodendroglial apoptosis in the developing brain.<sup>3–5</sup>

Apoptosis is the major type of cell death involved in development and tissue homeostasis to build up and maintain structural and functional organs. It is an important mechanism that determines the size, shape, and function of the vertebrate nervous system.<sup>6</sup> Two main pathways have a key role in the apoptotic program, namely, extrinsic and intrinsic apoptosis, which finally activate executioner caspases such as caspase-3, leading to characteristic features of this type of cell death, such as cell shrinkage, membrane blebbing, chromatin condensation, and DNA fragmentation.<sup>7</sup>

The extrinsic pathway is initiated by ligand-induced activation of specific death receptors of the tumor necrosis factor (TNF) superfamily, such as Fas, TNFR or TNF-related apoptosis-inducing ligand (TRAIL) at the plasma membrane.<sup>7</sup> There is a growing body of evidence that in the immature brain, Fas-dependent apoptosis is involved in experimental models of neonatal brain injury, such as hypoxia-ischemia,<sup>8</sup> infant head trauma,<sup>9</sup> and, as recently observed, after hyperoxic conditions.<sup>10</sup>

The second apoptotic pathway is mediated by intrinsic stress signals, such as DNA damage, oxidative stress or growth factor deprivation, and is characterized by the involvement of mitochondria.<sup>7,11</sup> Such stimuli induce the release of cytochrome *c* from the inner mitochondrial membrane into the cytosol. This release of cytochrome *c* is believed to be mediated by members of the pro-apoptotic B-cell lymphoma-2 (Bcl-2) family, such as Bcl-2-associated X protein (Bax), which is indispensable in the intrinsic apoptotic pathway. After a death signal, Bax activation,

<sup>1</sup>Department of Anaesthesiology and Intensive Care Medicine, Charité-Universitätsmedizin Berlin, Berlin, Germany; <sup>2</sup>Department of Neonatology, Charité-Universitätsmedizin Berlin, Berlin, Germany; <sup>3</sup>Department of Paediatrics I, Neonatology, University Hospital Essen, Essen, Germany; <sup>4</sup>Inserm U676, Hôpital Robert Debré, Paris, France; <sup>5</sup>Université Paris Diderot, UMR 676, Paris, France and <sup>6</sup>Department of Reproductive Biology, Imperial College London, Hammersmith Hospital, London, UK

\*Corresponding author: M Siffringer, Department of Anaesthesiology and Intensive Care Medicine, Charité-Universitätsmedizin Berlin, Campus Virchow-Klinikum D-13353, Berlin, Germany. Tel: +49 30 450 551 118; Fax +49 30 450 551 902; E-mail: marco.siffringer@charite.de

<sup>7</sup>These authors contributed equally to this work.

**Keywords:** caspase inhibitor; neonatal cell death; brain damage; hyperoxia; neuroprotection

**Abbreviations:** Apaf-1, apoptosis protease-activating factor-1; AIF, apoptosis-inducing factor; Bid, BH3-interacting domain death agonist; Bcl-2, B-cell lymphoma-2; TNF, tumor necrosis factor; Bax, Bcl-2-associated X protein; MOMP, mitochondrial outer membrane permeabilization; TRP601, 5-(2,6-difluoro-phenoxy)-3(R,S)-(2(S)-(2(S)-(3-methoxycarbonyl-2(S)-(3-methyl-2(S)-((quinoline-2-carbonyl)-amino)-butyrylamino)propionylamino)3-methylbutyrylamino)propionylamino)-4-oxo-pentanoic acid methyl ester

Received 30.8.11; revised 04.11.11; accepted 24.11.11; Edited by A Finazzi-Agrò

mediated by truncated Bcl-2 homology 3 (BH3)-only protein as BH3-interacting domain death agonist (Bid), leads to oligomerization and insertion to the lipid bilayer of the mitochondrial outer membrane, thereby initiating a channel-like structure that causes mitochondrial outer membrane permeabilization (MOMP), resulting in cytochrome *c* release.<sup>12</sup> Cytosolic cytochrome *c* binds to apoptosis protease-activating factor-1 (Apaf-1), and in the presence of ATP/dATP such complexes, which are called apoptosomes, can recruit and activate pro-caspase-9, leading to subsequent effector caspase (mostly caspase-3) activation that triggers apoptosis.<sup>13</sup> Through MOMP not only caspase-dependent but also caspase-independent apoptosis is initiated.<sup>14</sup> Apoptosis-inducing factor (AIF) was the first discovered protein that regulates caspase-independent apoptosis.<sup>15</sup> It was demonstrated that AIF is proteolytically released from mitochondria to the cytosol. Once in the cytosol, AIF translocates to the nucleus where it contributes to apoptosis.<sup>16</sup>

Although being one of the first discovered and most conserved caspases across mammals, the function of caspase-2 in apoptosis as an initiator or an executioner caspase has remained enigmatic for a long time.<sup>17</sup> However, it was demonstrated that caspase-2 is an initiator caspase involved in MOMP during apoptosis induced by several cellular insults, including heat shock, DNA damage, mitochondria oxidative stress, and cytoskeletal disruption.<sup>18–20</sup>

We investigated the effect of hyperoxia on the intrinsic apoptotic cascade by evaluating the expression of cytochrome *c*, Apaf-1, Bid, caspase-2, -3, the anti-apoptotic molecule Bcl-2. Additionally, we demonstrate that TRP601 (5-(2,6-difluoro-phenoxy)-3(R,S)-(2(S)-(2(S)-(3-methoxycarbonyl-2(S)-(3-methyl-2(S)-((quinoline-2-carbonyl)-amino)-butyrylamino)propionylamino)3-methylbutyrylamino)propionylamino)-4-oxo-pentanoic acid methyl ester), a pentapeptide-based caspase-2/caspase-3 inhibitor, which was recently published to protect the neonatal rodent brain against excitotoxicity, hypoxia-ischemia, and perinatal arterial stroke,<sup>21</sup> has a protective role in the context of hyperoxia. Furthermore, we provide evidence that hyperoxia triggers caspase-independent apoptosis by regulating AIF expression *in vivo*, which is also affected by TRP601.

## Results

**Hyperoxia mediates caspase-2 and -3 activation that is reduced by TRP601.** Using a preferential caspase-8 inhibitor, we have previously shown that caspase-8 is critically involved in Fas-mediated ‘extrinsic’ neuronal apoptosis after neonatal hyperoxia treatment.<sup>10</sup> To test whether the ‘intrinsic’ apoptotic pathway, suggested to be facilitated by caspase-2,<sup>20,22</sup> might also contribute to hyperoxia-mediated neonatal brain injury, we made use of a new pentapeptide caspase inhibitor designed to be a competitive and irreversible inhibitor (TRP601). Therefore, we performed initial *in vitro* experiments to determine the inhibitory capacity and specificity of TRP601. As shown in Figure 1a, TRP601 inhibits recombinant caspase-2 and -3 (Figure 1a). It should be noted that TRP601 is a pentapeptide derivative containing 2 methyl ester (OMe) groups on the

lateral chains of P1 and P4 aspartyl residues. As blood and cytoplasm of cells contain active esterase, these OMe groups of TRP601 are progressively removed after *in vivo* administration. We have synthesized this major metabolite ( $\Delta$ 2Me-TRP601) and evaluated its caspase-inhibitory capacity against recombinant caspase-2 and -3. Interestingly,  $\Delta$ 2Me-TRP601 is a very potent caspase-2 and -3 inhibitor ( $IC_{50/\Delta 2Me-TRP601/Casp2} \sim 7.4$  nM;  $IC_{50/\Delta 2Me-TRP601/Casp3} \sim 0.4$  nM; Figure 1b).

To characterize the functional consequences of inhibition by TRP601 *in vivo*, we determined cleaved caspase-2 expression and the enzymatic activity of caspase-2 and -3 in thalamic tissue. According to previous observations,<sup>10,23</sup> we detected an increase of caspase-3 activity, one of the main executioner caspases, in oxygen treated six-day-old rats after 12 h (186%) that peaks after 24 h (301%) of hyperoxia and that was ameliorated by TRP601 treatment (128% and 186%, respectively, Figure 1c). Of note, as revealed by protein expression of processed caspase-2 and enzymatic activity, compared with caspase-3, an even more significant increase was noted after 12 or 24 h of hyperoxia (364% and 649%, respectively, Figure 1d; 358% and 677%, respectively, Figure 1e, black bars), which was strongly reduced by TRP601 treatment (148% and 209%, respectively, Figure 1d; 125% and 250%, respectively, Figure 1e, gray bars), whereas TRP601 had no significant effect under normoxic conditions (dashed bars, Figure 1c–e).

**TRP601 attenuates neuronal cell death in the developing brain.** In line with the results of caspase-2 and -3 under hyperoxic conditions, neuronal cell death was significantly reduced after TRP601 treatment in cortex (frontal (II and IV), parietal (II and IV), cingulate (II and IV), and retrosplenial (II and IV)), caudate nucleus, corpus callosum and adjacent white matter, thalamus (laterodorsal, mediodorsal, and ventral nuclei), hippocampal dentate gyrus, and subiculum of rats treated for 24 h with 80% oxygen, as revealed by histological examination of Fluoro-Jade B-positive cells in 16 brain regions (Figure 2). The application of TRP601 under control conditions did not influence levels of physiological apoptosis (dashed *versus* white bar).

**Hyperoxia operates via intrinsic apoptosis in the developing rat brain.** As oxidative stress is one of the major causes of increased neural apoptosis in the developing brain under hyperoxic conditions,<sup>3,4,10,23,24</sup> we were interested in the regulation of protein expression of specific signaling molecules that are part of the mitochondria-dependent ‘intrinsic’ apoptotic pathway. These signaling pathway culminate in MOMP, and several previous studies have suggested that caspase-2 acts upstream of and initiating MOMP by direct processing of full-length Bid to activated truncated tBid.<sup>17</sup>

In this model, the analysis of full-length Bid in thalamic protein fraction by immunoblotting revealed a significant reduction of Bid after 12 and 24 h hyperoxia, suggesting a cleavage and subsequent activation of Bid (tBid), thereby providing a strong hint to the involvement of the intrinsic apoptotic pathway (Figure 3, black bars). Note, single application of the caspase-modulating agent (TRP601)

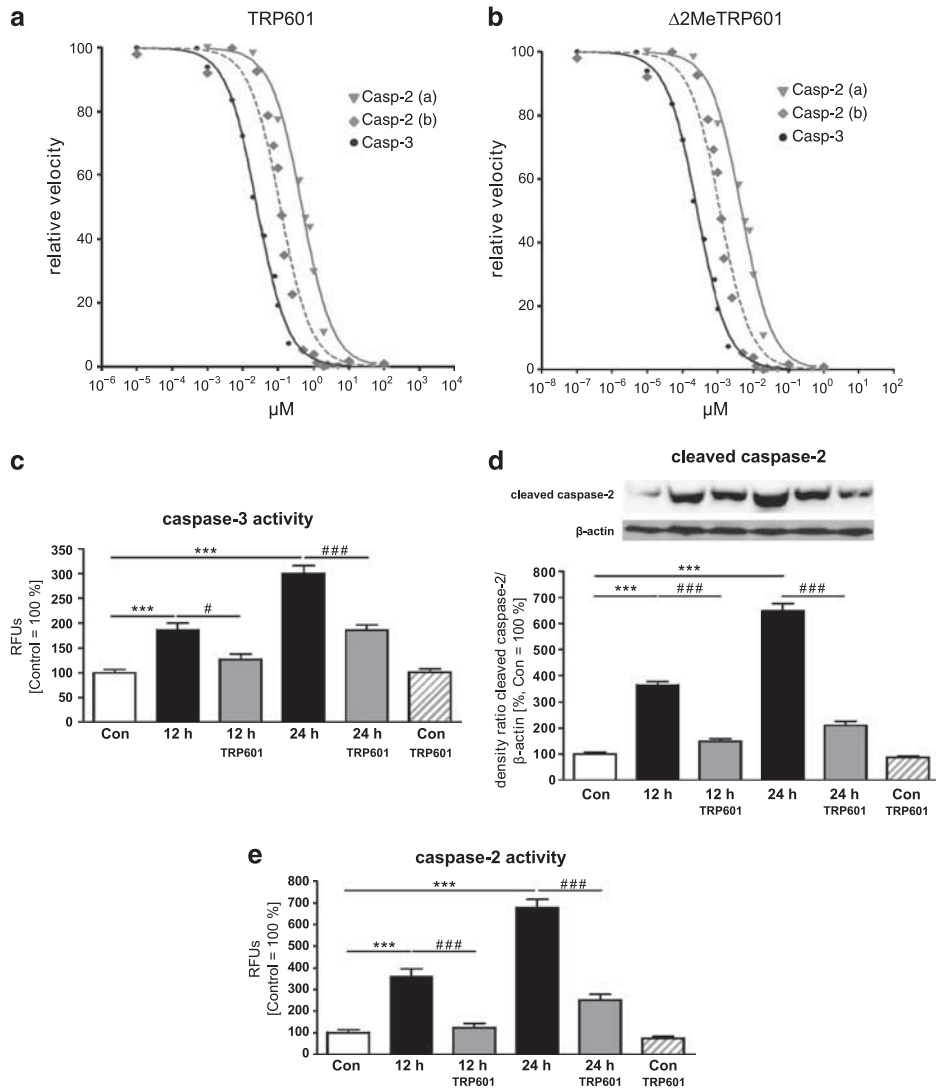


**Figure 1** Dose–response plots for inhibition of caspase-2 and -3 with TRP601 and its active metabolite. TRP601 (a) and Δ2Me-TRP601 (b) were added to recombinant caspase-2 (gray curves) and caspase-3 (black curves) to determine initial enzyme velocity and IC<sub>50</sub> values in chromogenic microplate assay. TRP601 and Δ2Me-TRP601 were added simultaneously to substrates (plain curves; IC<sub>50</sub>/TRP601/Casp3 = 25.58 ± 3.1 nM; IC<sub>50</sub>/Δ2Me-TRP601/Casp3 = 0.39 ± 0.11 nM; IC<sub>50</sub>/TRP601/Casp2(a) = 471.8 ± 91.3 nM; IC<sub>50</sub>/Δ2Me-TRP601/Casp2(a) = 7.4 ± 3.18 nM) or alternatively 45 min before substrates (dotted curves; IC<sub>50</sub>/TRP601/Casp2(b) = 115.2 ± 39.12 nM; IC<sub>50</sub>/Δ2Me-TRP601/Casp2(b) = 2.67 ± 1.46 nM). (c) Six-day-old Wistar rat pups were either injected with the caspase inhibitor TRP601 (1 mg/kg bodyweight, i.p.) or vehicle control before exposure to 80% O<sub>2</sub>. After 12 or 24 h, animals were killed, transcardially perfused with PBS, and brain samples were collected in order to perform a fluorometric caspase-3 activity assay. Measurements of hydrolysis of Ac-DEVD-AMC at 460 nm resulted in a highly significant upregulation of caspase-3 activity under hyperoxic conditions, whereas single treatment with TRP601 significantly decreased caspase-3 activity to control levels after 12 and 24 h. Bars represent mean ± S.E.M. (thalamus, n = 6/group, normalized to control animals (21% O<sub>2</sub>) \*\*\*P < 0.001, #P < 0.05, ###P < 0.001, two-way ANOVA). (d) Inhibition of caspase-2 by TRP601 *in vivo* (1 mg/kg bodyweight i.p.) lead to decreased protein expression of caspase-2 in thalamus from treated animals, whereas under normoxic conditions TRP601 had no effect. Data are normalized to levels of rat pups exposed to normoxia (control = 100%). Representative western blot images of caspase-2 and β-actin are shown for thalamus. Bars represent mean ± S.E.M. (n = 8/group, \*\*\*P < 0.001, ###P < 0.001, one-way ANOVA). (e) Six-day-old Wistar rat pups were either injected with the caspase inhibitor TRP601 (1 mg/kg bodyweight, i.p.) or vehicle control before exposure to 80% O<sub>2</sub>. After 12 or 24 h, animals were killed, transcardially perfused with PBS, and brain samples were collected in order to perform a fluorometric caspase-2 activity assay. Measurements of hydrolysis of VDVAD-AFC at 505 nm resulted in a highly significant upregulation of caspase-2 activity under hyperoxic conditions, whereas single treatment with TRP601 significantly decreased caspase-2 activity to control levels after 12 and 24 h. Bars represent mean ± S.E.M. (thalamus, n = 6/group, normalized to control animals (21% O<sub>2</sub>) \*\*\*P < 0.001, ###P < 0.001, two-way ANOVA)

restores nonactivated Bid in the cytosol (Figure 3, gray bars), the application of TRP601 generates no change under room air (normoxia, Figure 3, dashed bar). Furthermore, isolation of mitochondria and cytosolic protein fractions from six- to seven-day-old rat pups and subsequent western blot analysis showed that under hyperoxic conditions cytosolic cytochrome *c*

is increased, whereas it is decreased in mitochondria. The *in vivo* treatment with TRP601 reversed these hyperoxia-induced changes in subcellular cytochrome *c* distribution (Figure 4a). Densitometric analysis revealed highly significant differences in the hyperoxic and the treatment groups in both cellular fractions, whereas cytochrome *c* expression remains

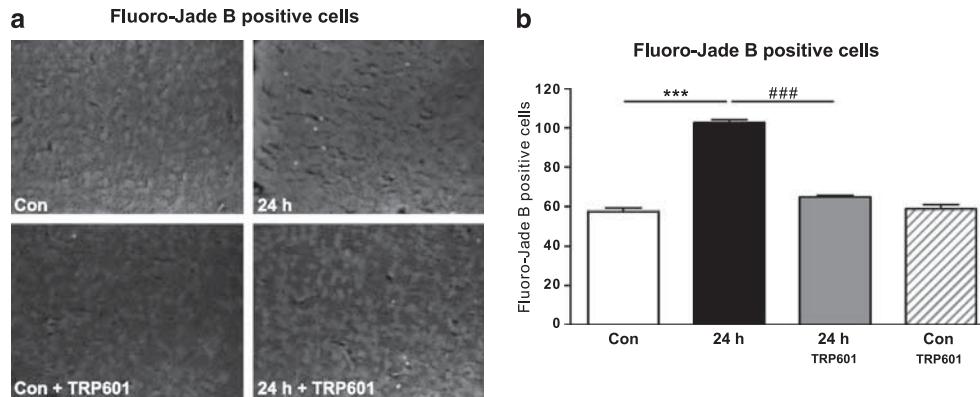


**Figure 2** TRP601 ameliorates neuronal cell death *in vivo*. (a) Representative photomicrographs (original magnification  $\times 400$ ) of Fluoro-Jade B-stained 10- $\mu$ m sections from the thalamus of seven-day-old rats, which were treated without or with TRP601 and were kept under room air (CON) or hyperoxic (24 h) conditions for 24 h. (b) Quantification of 16 brain regions indicates a highly significant reduction of Fluoro-Jade B-positive degenerated neurons after TRP601 treatment. Bars represent mean  $\pm$  S.E.M. ( $n = 8-12$ /group,  $***P < 0.001$ ,  $###P < 0.001$ , one-way ANOVA)

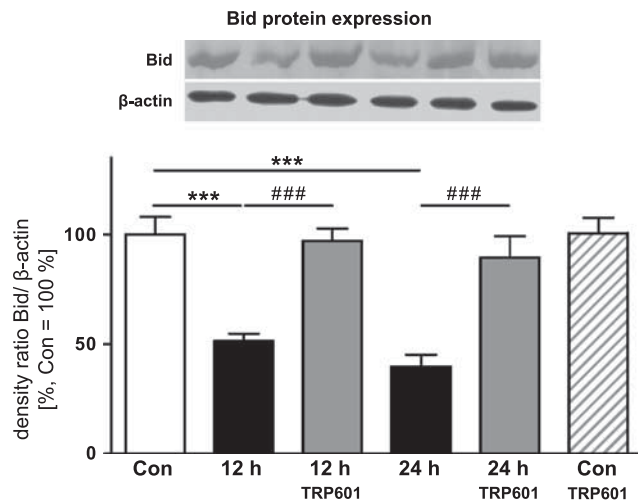


**Figure 3** Elevated oxygen concentrations induce Bid activation. Western blot from thalamic proteins and subsequent densitometric analysis of full-length Bid demonstrates a significant downregulation of Bid after hyperoxia (12 or 24 h, black bars), which is reversed by TRP601 treatment (gray bars, 1 mg/kg, i.p.), TRP601 under room air conditions showed no significant regulation (dashed bar). The densitometric data represent the ratio of the density of the Bid band to the corresponding  $\beta$ -actin band. Data are normalized to levels of rat pups exposed to normoxia (control = 100%; bars represent mean  $\pm$  S.E.M.,  $n = 7-9$ /group,  $***P < 0.001$ ,  $###P < 0.001$ , one-way ANOVA). Blots are representative of a series of three blots

comparable between treated and untreated animals under normoxic conditions (dashed *versus* white bar) in both cellular fractions (Figure 4a).

As cytochrome *c* forms a complex with Apaf-1 to recruit caspase-9 and builds up the so-called 'apoptosome',<sup>13</sup> we further investigated the effect of TRP601 on the regulation of Apaf-1 expression under hyperoxic conditions. By western blot and subsequent densitometric analysis, a highly significant upregulation of Apaf-1 protein expression after 12 and 24 h of hyperoxia was shown, decreasing to control levels by a single administration of TRP601 before hyperoxia. Treatment

with the caspase-2 and -3 inhibitors did not affect Apaf-1 expression under normoxic conditions (Figure 4b).

**Hyperoxia results in downregulation of Bcl-2.** Members of the Bcl-2-superfamily are known to be specific regulators of not only caspase-dependent but also -independent apoptotic signaling pathways,<sup>12</sup> and are shown to be regulated in neonatal brain injury.<sup>9,11</sup> We investigated whether there are changes in response to hyperoxia in the expression of the anti-apoptotic protein Bcl-2, and whether TRP601 has an influence in this experimental setting. As revealed by quantitative real-time PCR (Figure 5a), 12 and 24 h of hyperoxia caused a significant decrease in Bcl-2 mRNA expression, whereas TRP601 treatment increased the expression almost to control levels. There was a slight increase in Bcl-2 mRNA expression under normoxic conditions (111% *versus* 101%), which did not reach statistical significance. The analysis and densitometric quantification of protein expression detected by immunoblotting revealed similar regulation patterns but showed no increase in protein expression of Bcl-2 under normoxic conditions (Figure 5b).

**Hyperoxia triggers (caspase independent) AIF release into the cytosol.** The neuronal cell death program is tightly regulated and mostly performed by caspases. To check whether TRP601 functions exclusively through inhibition of caspase-mediated apoptosis, we further investigated a caspase-independent apoptosis pathway that is mainly mediated by AIF.<sup>15,16</sup> Therefore, protein expression of AIF in brain lysates of TRP601 or vehicle-treated pups, which have been exposed to either 21 or 80% oxygen after treatment, was measured. Western blot analysis and quantification of thalamic AIF protein expression revealed a significant upregulation after hyperoxia, whereas TRP601 administration reversed this effect (Figure 6). The physiological AIF expression did not change after TRP601 treatment in seven-day-old rat pups under control conditions (Figure 6, dashed *versus* white bar).



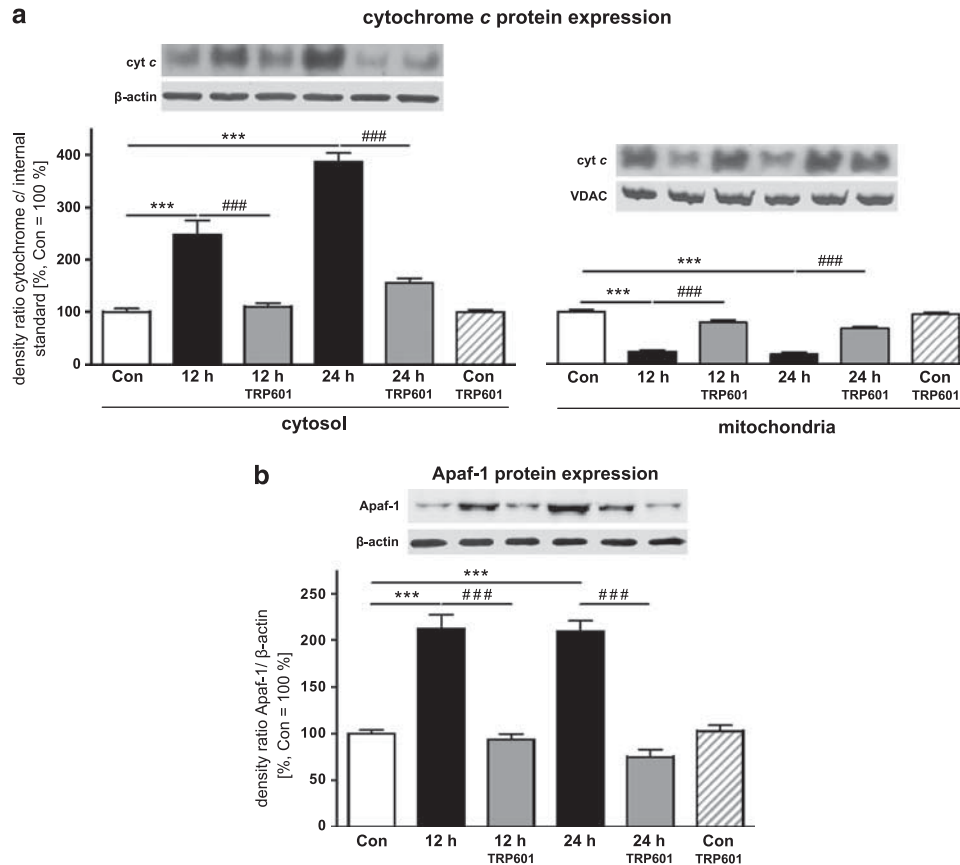


**Figure 4** TRP601 treatment inhibits hyperoxia-induced intrinsic apoptosis. (a) Western blot analysis from thalamic cytosolic and mitochondrial protein fractions implies a shift of cytochrome c from mitochondria to the cytosol under hyperoxic conditions that could be prevented by a single TRP601 treatment (1 mg/kg, i.p.). (b) Western blot analysis of Apaf-1 expression in thalamic brain samples displays a significant upregulation after 12 and 24 h hyperoxia, which was blocked by TRP601. The densitometric data represent the density ratio of relevant individual bands to the corresponding internal standard band ( $\beta$ -actin or VDAC). Data are normalized to levels of rat pups exposed to normoxia (control 100%; bars represent mean  $\pm$  S.E.M.,  $n = 6$ /group, \*\*\* $P < 0.001$ , ### $P < 0.001$ , one-way ANOVA compared with respective controls). Blots are representative of a series of three blots

## Discussion

The present study reveals the involvement of caspase-2 in combination with the intrinsic apoptotic cascade in hyperoxia-induced injury to the immature central nervous system. We report for the first time that the inhibitor TRP601 provides strong evidence for neuroprotective action against hyperoxia-induced apoptosis influencing intrinsic caspase-dependent and also caspase-independent pathways. Our results are in line with a recently published report of a protective effect of TRP601 in other rodent models of perinatal rodent brain injury,<sup>21</sup> and suggest different potential molecular mechanisms that may entertain this tissue-protective effect of TRP601.

**Hyperoxia-induced caspase activation is reduced by TRP601.** To determine the inhibitory capacity and specificity of TRP601, we first tested TRP601 *in vitro*. TRP601 and its active metabolite  $\Delta 2$ Me-TRP601 are potent inhibitors of caspase-2 and -3. This correlates with elegant *in vitro* studies using VDVAD-based substrates and inhibitors.<sup>25,26</sup>

Caspase-2 has been recognized as an initiator caspase in neuronal apoptosis during  $\beta$ -amyloid-mediated toxicity,<sup>27</sup>

serum deprivation,<sup>28</sup> and oxidative stress-induced apoptosis of neuronal stem cells.<sup>29</sup> In our experimental setting, hyperoxia mediates caspase-2 activation that is reduced by TRP601. Previous studies in different animal models of oxygen toxicity<sup>4,10,23,30</sup> revealed a significant increase of effector caspase-3 activity in the brain of oxygen-treated animals. Treatment with TRP601 highly ameliorates enzymatic caspase-3 activity. Our *in vivo* results suggest that TRP601 might function upstream of caspase-3; this is supported by previous reports demonstrating *in vitro* and *in vivo* the inhibition of caspase-3 activity downstream of caspase-2 modulation with siRNA and caspase-2-deficient mice.<sup>28,31</sup> However, our data do not exclude the possibility that the TRP601 protective effects might be mediated, at least in part, through a direct effect of caspase-3.

**TRP601 attenuates neuronal cell death in the developing brain.** Exposure of infant rats (P6) to a high oxygen concentration of 80% over a period of 24 h increased the rate of cell death in the developing rat brain acutely (see Figure 2). In previous studies, we demonstrated that hyperoxia-induced cell death displays morphological features of physiological apoptotic cell death, occurs in a

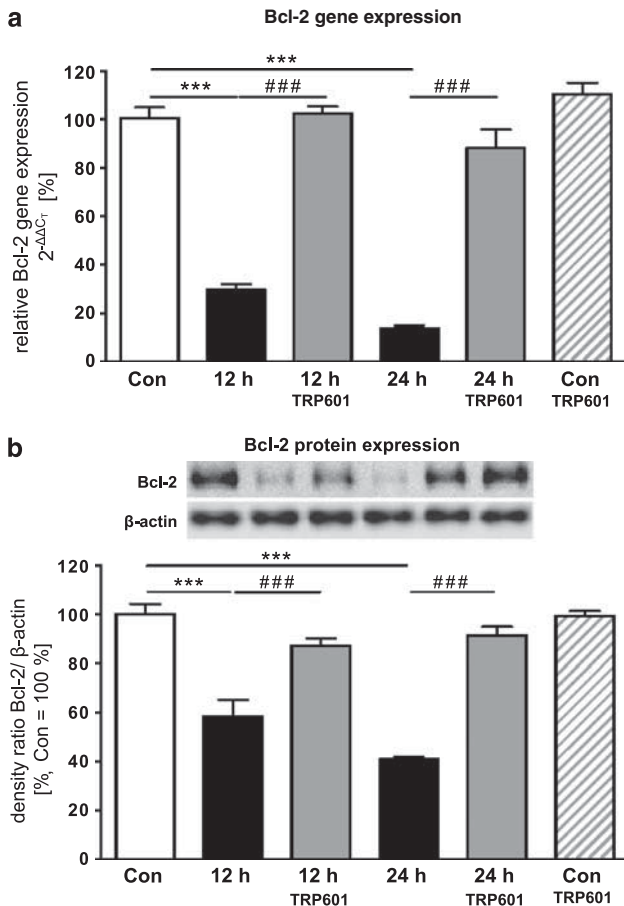


**Figure 5** TRP601 restores Bcl-2 expression under hyperoxic conditions. (a) Quantitative analysis of mRNA expression by real-time PCR showed a marked reduction of Bcl-2 mRNA expression in thalamic samples of rat pups that were kept for 12 and 24 h under hyperoxia (black bars), whereas TRP601 treatment restores Bcl-2 expression to control levels (gray bars). Application of TRP601 under room air (control, dashed bar) showed no significant regulation on Bcl-2 mRNA expression. (b) The analysis of Bcl-2 protein expression by western blot showed a similar expression pattern. The protein expression of Bcl-2 is significantly decreased after 12 and 24 h; the single application of TRP601 could restore the Bcl-2 protein expression almost up to control level. The densitometric data represent the ratio of the density of the Bcl-2 band to the corresponding  $\beta$ -actin band. Data are normalized to levels of rat pups exposed to normoxia (control 100%; bars represent mean  $\pm$  S.E.M., thalamus,  $n = 6$ –8/group,  $***P < 0.001$ ,  $###P < 0.001$ , one-way ANOVA compared with respective controls). Blots are representative of a series of three blots

disseminated fashion throughout the immature rat brain, is age dependent, and affects rodents most severely in the first week of life.<sup>23,24</sup> A significant decrease of cell death was detected when rats were treated intraperitoneally with 1 mg/kg TRP601 before exposure to high oxygen levels. This effect indicates possible therapeutic implications of TRP601 in neonatal medicine as a preventive neuroprotective agent. In line with our results, a neuroprotective effect of apoptosis-modulating agents has been reported in various *in vivo* and *in vitro* neonatal experimental models.<sup>21,31,32</sup>

**TRP601 inhibits intrinsic apoptotic signaling.** Caspase-2 has been shown to induce MOMP that leads to the release of pro-apoptotic molecules from mitochondria as the release of

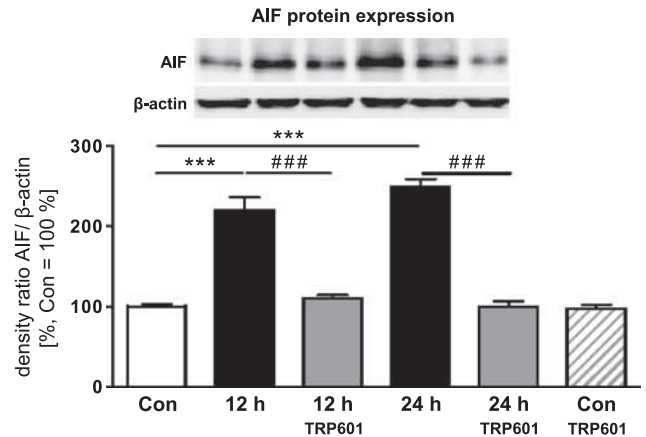


**Figure 6** Caspase-independent hyperoxia-induced apoptosis is regulated by TRP601 treatment. Densitometric quantification of AIF expression by western blotting demonstrates a significant upregulation of AIF expression in thalamic samples of hyperoxia-treated rat pups after 12 and 24 h, which is prevented by TRP601 treatment. The densitometric data represent the ratio of the density of the AIF band to the corresponding  $\beta$ -actin band. Data are normalized to levels of rat pups exposed to normoxia (control 100%; bars represent mean  $\pm$  S.E.M.;  $n = 6$ /group,  $***P < 0.001$ ,  $###P < 0.001$ , one-way ANOVA compared with respective controls). Blots are representative of a series of three blots

cytochrome *c*.<sup>13,18,22</sup> A key step in this mitochondrial intrinsic pathway of apoptosis is the interaction of members of the Bcl-2 family to permeabilize the mitochondrial outer membrane as indicated in several studies.<sup>12</sup> To further elucidate mechanisms involved in the reduction of apoptosis by TRP601, we visualized cytochrome *c* and Bcl-2 expression levels after hyperoxia and TRP601 treatment. Our indirect observation of MOMP as shown by a shift of cytochrome *c* from the mitochondrion to the cytosol and a decrease in full-length Bid coincides with a drastic reduction of Bcl-2 on mRNA and protein expression. This decrease in Bcl-2 expression might rearrange the balance between pro- and anti-apoptotic Bcl-2 family members toward apoptosis, and trigger the release of cytochrome *c* most probably by activation of Bid and consecutive pore-forming ability of Bax to the outer mitochondrial membrane.<sup>33</sup> However, the underlying mechanism how TRP601 'stabilizes' Bcl-2 expression needs to be clarified by future investigations. The precise mechanism involved is controversial. Nonetheless, several models have been proposed in which Bid and Bcl-2 interact.<sup>34,35</sup>

Apaf-1 has been described as the core of the apoptosome, and in the developing brain, Apaf-1 is a death regulator of neural precursor cells.<sup>13,36</sup> Noteworthy, in our model of oxygen toxicity, Apaf-1 levels increased under hyperoxic conditions and single TRP601 treatment diminished this upregulation, and seems to be a part of the protective mechanism of TRP601. Interestingly, inhibition of Apaf-1 signaling pathway downstream of mitochondrial damage confers neuroprotection in a rodent model of neonatal hypoxic-ischemic brain injury.<sup>37</sup>

**Hyperoxia triggers AIF release into the cytosol.** Despite the fact that AIF is proteolytically released from the

intermitochondrial membrane post-MOMP to the cytoplasm, once in the cytosol it translocates to the nucleus where it induces typical features of apoptosis.<sup>15,16</sup> However, recently the existence of a pool of AIF at the outer mitochondrial membrane (cytosolic site) with the ability to readily translocate to the nucleus upon excitotoxic stimuli was demonstrated.<sup>38</sup> Here, we showed a significant upregulation of cytosolic protein expression of mature AIF, which was totally blocked by a single treatment with TRP601. *In vivo* studies consistently demonstrate that AIF targeting has a large effect on neurons. AIF can be beneficial or harmful for neurons, depending on physiological settings.<sup>39,40</sup>

To our knowledge, this is the first report elucidating the direct effects of neonatal hyperoxia in the developing rat brain, which specifically focuses on intrinsic apoptosis and investigates a promising neuroprotective substance (TRP601). The present study shows that caspase-2 has a role upstream of the mitochondrial pathway, and TRP601 can prevent MOMP.

Our data suggest that caspase-2 and -3 may be therapeutic targets to limit neurodegeneration resulting from hyperoxia-induced injury in the developing brain. Our findings are highly relevant from a clinical perspective because oxygen administration to neonates is often inevitable and candidates for adjunctive neuroprotective therapies are still missing.

## Materials and Methods

**Preparation of drug solutions.** For *in vitro* studies, TRP601 (C<sub>40</sub>H<sub>48</sub>F<sub>2</sub>N<sub>6</sub>O<sub>11</sub>; MW: 826.84; Chiesi, Parma, Italy) and  $\Delta$ 2Me-TRP601 (C<sub>38</sub>H<sub>44</sub>F<sub>2</sub>N<sub>6</sub>O<sub>11</sub>; MW: 798.79) were initially solubilized in 100% DMSO. The final concentration of DMSO was  $\leq$  10%. For *in vivo* experiments, TRP601 was formulated in 0.9% NaCl containing 0.1% DMSO for intraperitoneal (i.p.) administration, an appropriate vehicle control (0.1% DMSO in 0.9% NaCl) was used for control animals as indicated.

***In vitro* enzyme kinetics.** Kinetics experiments were done according to the continuous method. Assays of chromogenic substrate cleavage contained in 100  $\mu$ l caspase buffer (20 mM HEPES, pH 7.4, 0.1% CHAPS, 5 mM DTT, 2 mM EDTA), 58.5 ng of human active recombinant caspase-2 (Biomol, Plymouth, MN, USA) or 20 ng of human active recombinant caspase-3 (Sigma, Saint Louis, MO, USA), and 100  $\mu$ M of chromogenic substrate (Ac-DEVD-pNA for caspase-3 and Ac-VDVAD-pNA for caspase-2) in the presence of a range of concentrations of TRP601 or  $\Delta$ 2ME-TRP601. For caspase-2 assays, buffer was supplemented with 1 M succinate. Cleavage of the chromogenic substrate as a function of time was monitored at 405 nm, and the initial velocity ( $V_0$ ) was determined from the linear portion of the progress curve. The formation of para-nitroaniline (pNA) was followed every 30 s for 150 min at 37 °C with a microtiter plate reader (Paradigm Multi-Mode Microplate Detection Platform, SoftMax Pro 5.2 software; Molecular Devices, St. Grégoire, France).  $V_0$ , relative velocities, Km, and IC<sub>50</sub> were determined from experimental data using GraphPad Prism 5.01 software program (GraphPad Software, La Jolla, CA, USA). Standard deviations of the reported values were below 10%.

**Animal experiments.** Six-day-old Wistar rats (Charité-Universitätsmedizin Berlin) were randomly assigned to four groups and treated as follows: (1) normoxia (21% O<sub>2</sub>) and vehicle i.p. injections, (2) normoxia and 1 mg TRP601/kg i.p. injections, (3) hyperoxia (80% O<sub>2</sub>) and vehicle i.p. injections, and (4) hyperoxia and 1 mg TRP601/kg i.p. injections. For hyperoxia or normoxia exposure, pups were kept with their dams. In all study groups, TRP601 or vehicle was injected at the beginning of an oxygen/room air exposure.

Animal experiments were performed according to institutional guidelines of the Charité-Universitätsmedizin Berlin.

**Tissue preparation.** At 12 and 24 h after treatment initiation, postnatal day-6 (P6) Wistar rat pups were killed with chloral hydrate (1 mg/kg, i.p.). For histological

analysis, P6 Wistar rat pups ( $n=6$  per group) were transcardially perfused with heparinized 0.01 M phosphate-buffered saline at pH 7.4, subsequently with 4% paraformaldehyde at pH 7.4, and decapitated. Brains were removed, the cerebellum and the olfactory bulb discarded. After a postfixation time of 3 days at 4 °C, brains were embedded in paraffin and processed for Fluoro-Jade B staining. For molecular studies, P6 Wistar rat pups ( $n=6-10$  per group) were transcardially perfused with normal saline solution and decapitated. Brain tissue was microdissected from the retrosplenial cortex and thalamus, snap frozen in liquid nitrogen, and stored at  $-80$  °C.

**Fluoro-Jade B staining and quantitation of neurodegeneration in different brain regions.** Paraffin sections (10  $\mu$ m) were stained with Fluoro-Jade B, and degenerating cells were determined in the frontal, parietal, cingulate, retrosplenial cortex, caudate nucleus, corpus callosum and adjacent white matter, thalamus, hippocampal dentate gyrus, and subiculum by means of a stereological dissector estimating mean numerical cell densities of degenerating cells as described previously.<sup>3</sup>

**Quantitative real-time PCR.** Total cellular RNA was isolated from snap-frozen tissue by acidic phenol/chloroform extraction and reverse transcribed. The resulting cDNA was amplified by real-time PCR. Real-time PCR for *Bcl-2* was performed in triplicates for each sample using 20  $\times$  Assays-on-Demand Gene Expression Assay Mix (Applied Biosystems, Foster City, CA, USA) and 30 ng of cDNA template. For hypoxanthine-guanine phosphoribosyltransferase (*HPRT*), the PCR reaction was carried out with 150 pg cDNA. The expression of *Bcl-2* and *HPRT* was analyzed with the ABI Prism 7500 sequence detection system (Applied Biosystems) according to standard 2<sup>- $\Delta\Delta$ CT</sup> method.

**Immunoblotting.** Western blot analysis was performed as published elsewhere,<sup>3</sup> with minor adaptations. Briefly, nitrocellulose membranes were incubated overnight at 4 °C with rabbit polyclonal anti-caspase-2 (18 kDa; 1 : 200; Santa Cruz Biotechnology, Santa Cruz, CA, USA), anti-cytochrome *c* (12.6 kDa; 1 : 1.000; BioVision, Mountain View, CA, USA), anti-Apaf-1 (135 kDa; 1 : 500; New England Biolabs, Frankfurt, Germany), anti-Bid (22 kDa; 1 : 1.000; Millipore, Schwalbach, Germany), or anti-AIF (57 kDa; 1 : 500; New England Biolabs). Secondary incubations were performed with horseradish peroxidase-linked anti-rabbit antibody (1 : 5.000; Amersham Biosciences, Bucks, UK). Positive signals were visualized using enhanced chemiluminescence (Amersham Biosciences) and quantified using a ChemiDoc XRS + system and the software Quantity One (Bio-Rad, Munich, Germany). Membranes were stripped, then washed, blocked, and reprobed overnight at 4 °C with mouse anti- $\beta$ -actin monoclonal antibody (42 kDa; 1 : 10.000; Sigma-Aldrich, Taufkirchen, Germany) or anti-voltage-dependent anion channel (VDAC) polyclonal antibody (32 kDa; 1 : 1.000; New England Biolabs).

**Measurement of caspase-2 and -3 enzymatic activities.** Caspase-2 and -3 activities were measured using fluorometric assay kits (BioVision and Sigma-Aldrich). Protein samples were prepared as described for western blotting by using the lysis buffer of the kit, and the samples were incubated with the fluorogenic substrates VDAD-AFC (caspase-2) or Ac-DEVD-AMC (caspase-3). The enzymatic activity was measured using an Infinite M200 fluorescent plate reader (Tecan, Salzburg, Austria).

**Statistical analyses.** Data were analyzed using the R Project for Statistical Computing (Statistics Department of the University of Auckland, Auckland, New Zealand) and presented as mean  $\pm$  standard error. Group effects were assessed by analysis of variance (ANOVA), followed by *post hoc* independent sample *t*-test multiple comparison. *P*-values are presented after Bonferroni correction. Adjusted *P*-values of  $<0.05$  were considered statistically significant.

## Conflict of Interest

The authors declare no conflict of interest.

**Acknowledgements.** We apologize to those colleagues whose papers were not cited because of a strict reference limit. This work was supported by grants from the European Commission (Sixth Framework Program, contract no LSHM-CT-2006-036534), the Sonnenfeld Stiftung, Berlin, Inserm (France), Medical Research Council (UK, P19381), and the Stiftung Universitätsmedizin Essen.

1. Johnson S, Wolke D, Hennessy E, Marlow N. Educational outcomes in extremely preterm children: neuropsychological correlates and predictors of attainment. *Dev Neuropsychol* 2011; **36**: 74–95.
2. Keller M, Felderhoff-Mueser U, Lagercrantz H, Dammann O, Marlow N, Hüppi P *et al*. Policy benchmarking report on neonatal health and social policies in 13 European countries. *Acta Paediatr* 2010; **99**: 1624–1629.
3. Felderhoff-Mueser U, Siffringer M, Polley O, Dziatko M, Leineweber B, Mahler L *et al*. Caspase-1-processed interleukins in hyperoxia-induced cell death in the developing brain. *Ann Neurol* 2005; **57**: 50–59.
4. Gerstner B, Siffringer M, Dziatko M, Schüller A, Lee J, Simons S *et al*. Estradiol attenuates hyperoxia-induced cell death in the developing white matter. *Ann Neurol* 2007; **61**: 562–573.
5. Schmitz T, Ritter J, Mueller S, Felderhoff-Mueser U, Chew L-J, Gallo V. Cellular changes underlying hyperoxia-induced delay of white matter development. *J Neurosci* 2011; **31**: 4327–4344.
6. Kuan CY, Roth KA, Flavell RA, Rakic P. Mechanisms of programmed cell death in the developing brain. *Trends Neurosci* 2000; **23**: 291–297.
7. Jin Z, El-Deiry WS. Overview of cell death signaling pathways. *Canc Biol Ther* 2005; **4**: 139–163.
8. Northington FJ, Ferriero DM, Graham EM, Traystman RJ, Martin LJ. Early neurodegeneration after hypoxia-ischemia in neonatal rat is necrosis while delayed neuronal death is apoptosis. *Neurobiol Dis* 2001; **8**: 207–219.
9. Felderhoff-Mueser U, Siffringer M, Pedsitschek S, Kuckuck H, Moysich A, Bittigau P *et al*. Pathways leading to apoptotic neurodegeneration following trauma to the developing rat brain. *Neurobiol Dis* 2002; **11**: 231–245.
10. Dziatko M, Boos V, Siffringer M, Polley O, Gerstner B, Genz K *et al*. A critical role for Fas/CD-95 dependent signaling pathways in the pathogenesis of hyperoxia-induced brain injury. *Ann Neurol* 2008; **64**: 664–673.
11. Hagberg H, Mallard C, Rousset CI, Xiaoyang W. Apoptotic mechanisms in the immature brain: involvement of mitochondria. *J Child Neurol* 2009; **24**: 1141–1146.
12. Chipuk JE, Moldoveanu T, Lambl F, Parsons MJ, Green DR. The BCL-2 family reunion. *Mol Cell* 2010; **37**: 299–310.
13. Bao Q, Shi Y. Apoptosome: a platform for the activation of initiator caspases. *Cell Death Differ* 2007; **14**: 56–65.
14. Kroemer G, Galluzzi L, Brenner C. Mitochondrial membrane permeabilization in cell death. *Physiol Rev* 2007; **87**: 99–163.
15. Susin SA, Lorenzo HK, Zamzami N, Marzo I, Snow BE, Brothers GM *et al*. Molecular characterization of mitochondrial apoptosis-inducing factor. *Nature* 1999; **397**: 441–446.
16. Otera H, Ohsakaya S, Nagaura Z-I, Ishihara N, Mihara K. Export of mitochondrial AIF in response to proapoptotic stimuli depends on processing at the intermembrane space. *EMBO J* 2005; **24**: 1375–1386.
17. Kumar S. Caspase 2 in apoptosis, the DNA damage response and tumour suppression: enigma no more? *Nat Rev Cancer* 2009; **9**: 897–903.
18. Bouchier-Hayes L, Oberst A, McStay GP, Connell S, Tait SW, Dillon CP *et al*. Characterization of cytoplasmic caspase-2 activation by induced proximity. *Mol Cell* 2009; **35**: 830–840.
19. Ho LH, Read SH, Dorstyn L, Lambrusco L, Kumar S. Caspase-2 is required for cell death induced by cytoskeletal disruption. *Oncogene* 2008; **27**: 3393–3404.
20. Tiwari M, Lopez-Cruzan M, Morgan WW, Herman B. Loss of caspase-2-dependent apoptosis induces autophagy after mitochondrial oxidative stress in primary cultures of young adult cortical neurons. *J Biol Chem* 2011; **286**: 8493–8506.
21. Chauvier D, Renolleau S, Holifanjaniaina S, Ankré S, Bezault M, Schwendemann L *et al*. Targeting neonatal ischemic brain injury with a pentapeptide-based irreversible caspase inhibitor. *Cell Death Dis* 2011; **2**: e203.
22. Guo Y, Srinivasula SM, Druihne A, Fernandes-Alnemri T, Alnemri ES. Caspase-2 induces apoptosis by releasing proapoptotic proteins from mitochondria. *J Biol Chem* 2002; **277**: 13430–13437.
23. Kaindl AM, Siffringer M, Koppelstaetter A, Genz K, Loeber R, Boerner C *et al*. Erythropoietin protects the developing brain from hyperoxia-induced cell death and proteome changes. *Ann Neurol* 2008; **64**: 523–534.
24. Felderhoff-Mueser U, Bittigau P, Siffringer M, Jarosz B, Korobowicz E, Mahler L *et al*. Oxygen causes cell death in the developing brain. *Neurobiol Dis* 2004; **17**: 273–282.
25. Pereira NA, Song Z. Some commonly used caspase substrates and inhibitors lack the specificity required to monitor individual caspase activity. *Biochem Biophys Res Commun* 2008; **377**: 873–877.
26. Talanian RV, Quinlan C, Trautz S, Hackett MC, Mankovich JA, Banach D *et al*. Substrate specificities of caspase family proteases. *J Biol Chem* 1997; **272**: 9677–9682.
27. Troy CM, Rabacchi SA, Friedman WJ, Frappier TF, Brown K, Shelanski ML. Caspase-2 mediates neuronal cell death induced by beta-amyloid. *J Neurosci* 2000; **20**: 1386–1392.
28. Chauvier D, Lecœur H, Langonné A, Borgne-Sanchez A, Mariani J, Martinou JC *et al*. Upstream control of apoptosis by caspase-2 in serum-deprived primary neurons. *Apoptosis* 2005; **10**: 1243–1259.
29. Tamm C, Zhivotovsky B, Ceccatelli S. Caspase-2 activation in neural stem cells undergoing oxidative stress-induced apoptosis. *Apoptosis* 2008; **13**: 354–363.
30. Solberg R, Löberg EM, Andresen JH, Wright MS, Charrat E, Khrestchatsky M *et al*. Resuscitation of newborn piglets. short-term influence of FIO<sub>2</sub> on matrix metalloproteinases, caspase-3 and BDNF. *PLoS One* 2010; **5**: e14261.
31. Carlsson Y, Schwendemann L, Vontell R, Rousset CI, Wang X, Lebon S *et al*. Genetic inhibition of caspase-2 reduces hypoxic-ischemic and excitotoxic neonatal brain injury. *Ann Neurol* 2011 accepted for publication.
32. Nijboer CH, Heijnen CJ, van der Kooij MA, Zijlstra J, van Velthoven CT, Culmsee C *et al*. Targeting the p53 pathway to protect the neonatal ischemic brain. *Ann Neurol* 2011; **70**: 255–264.
33. Brustovetsky T, Li T, Yang Y, Zhang JT, Antonsson B, Brustovetsky N. BAX insertion, oligomerization, and outer membrane permeabilization in brain mitochondria: role of permeability transition and SH-redox regulation. *Biochim Biophys Acta* 2010; **1797**: 1795–1806.
34. Ding J, Zhang Z, Roberts GJ, Falcone M, Miao Y, Shao Y *et al*. Bcl-2 and Bax interact via the BH1-3 groove-BH3 motif interface and a novel interface involving the BH4 motif. *J Biol Chem* 2010; **285**: 28749–28763.
35. Tan C, Dlugosz PJ, Peng J, Zhang Z, Lapolla SM, Pfaffner SM *et al*. Auto-activation of the apoptosis protein Bax increases mitochondrial membrane permeability and is inhibited by Bcl-2. *J Biol Chem* 2006; **281**: 14764–14775.
36. D'Sa C, Klocke BJ, Ceconi F, Lindsten T, Thompson CB, Korsmeyer SJ *et al*. Caspase regulation of genotoxin-induced neural precursor cell death. *J Neurosci Res* 2003; **74**: 435–445.
37. Gao Y, Liang W, Hu X, Zhang W, Stetler RA, Vosler P *et al*. Neuroprotection against hypoxic-ischemic brain injury by inhibiting the apoptotic protease activating factor-1 pathway. *Stroke* 2010; **41**: 166–172.
38. Yu S-W, Wang Y, Frydenlund DS, Ottersen OP, Dawson VL, Dawson TM. Outer mitochondrial membrane localization of apoptosis-inducing factor: mechanistic implications for release. *ASN Neuro* 2009; **1**: e00021.
39. Engel T, Plesnila N, Prehn JH, Henshall DC. *In vivo* contributions of BH3-only proteins to neuronal death following seizures, ischemia, and traumatic brain injury. *J Cereb Blood Flow Metab* 2011; **31**: 1196–1210.
40. Sevríoukova IF. Apoptosis-inducing factor: structure, function, and redox regulation. *Antioxid Redox Signal* 2011; **14**: 2545–2579.



**Cell Death and Disease** is an open-access journal published by Nature Publishing Group. This work is licensed under the Creative Commons Attribution-NonCommercial-No Derivative Works 3.0 Unported License. To view a copy of this license, visit <http://creativecommons.org/licenses/by-nc-nd/3.0/>